

Study of some thermal and mechanical properties of magnesium aluminium silicate glass ceramic

Madhumita Goswami^a, A. Sarkar^a, T. Mirza^a, V.K. Shrikhande^a, Sangeeta^a,
K.R. Gurumurthy^b, G.P. Kothiyal^{a,*}

^aTechnical Physics and Prototype Engineering Division, Bhabha Atomic Research Centre, Mumbai-400 085, India

^bAtomic Fuels Division, Bhabha Atomic Research Centre, Mumbai-400 085, India

Received 16 July 2001; received in revised form 13 August 2001; accepted 26 November 2001

Abstract

Magnesium aluminium silicate glass ceramics having different amounts of magnesium fluoride (nucleant) in the range 0–13.2 mol%, have been prepared by following the glass route (bulk nucleation). The base glass and glass ceramic samples were characterized by X-ray diffraction (XRD), thermal expansion coefficient (TEC), glass transition temperature (T_g), micro hardness, scanning electron microscopy measurements. Thermal expansion coefficient, T_g , and micro hardness of the base glass and glass ceramic samples are seen to be interdependent but due to the multi-component system the behaviour is seen to be somewhat complex. The average TEC (30–300 °C) and T_g of base glass samples decrease from 8.38 to $7.936 \times 10^{-6}/^{\circ}\text{C}$, and from 653.55 to 599.8 °C, respectively, with an increase in MgF_2 content. XRD measurements revealed the formation of different phases such as magnesium silicate, fluorophlogopite, nobergite etc. at different processing temperatures (max. 1050 °C). In all the cases thermal expansion coefficient increases and micro hardness decreases when glass is transformed to glass ceramic by controlled crystallization. The present studies show that the thermal expansion coefficient, T_g and micro hardness of the base glass depend, among other parameters, on the Mg concentration in the glass matrix, whereas they depend on the type of crystalline phases along with microstructure for the glass ceramic samples. © 2002 Elsevier Science Ltd and Techna S.r.l. All rights reserved.

Keywords: C. Thermal and mechanical properties; Magnesium aluminium silicate glass ceramics

1. Introduction

The glass ceramics based on the magnesium aluminium silicate (MAS) system belong to an important class of advanced technological material, having a wide range of applications [1–3]. Some of their interesting features are machinability, high thermal stability, high electrical insulation, vacuum compatibility etc. Various properties of MAS glass ceramics like hardness, expansion coefficient, conductivity and machinability etc., among other parameters, depend on the composition and microstructure. Recently some studies on the effect of aspect ratio of mica crystals and crystallinity on the micro hardness and machinability on glass ceramics

were reported by Baik et al. [4]. The crystal morphology in mica glass ceramics has also been studied by Hoche et al. [5]. In fact, the good machinability of MAS glass ceramic arises as a result of a special microstructure having tiny crystals dispersed uniformly throughout the glassy matrix. Habelitz et al. [6] carried out some investigations to see the effect of crystal orientation on the mechanical properties of mica glass ceramic. These machinable glass ceramics can be machined to precise tolerance and surface finish with conventional techniques. Radonjic and Nikolic [7] studied the effect of the fluorine content and its source on the crystallization of this class of ceramic materials. They have identified the predominant crystalline phases as fluorite, norbergite or fluorophlogopite depending on fluorine concentration, the heat treatment etc.

While electrical conductivity, machinability, outgassing properties are important for applications involving high voltage and ultra high vacuum, the knowledge of thermal and mechanical properties of glass ceramic is

* Corresponding author. Fax: +91-22-5505151.

E-mail address: gpkoth@apsara.barc.ernet.in (G.P. Kothiyal).

needed for the applications in the field of glass ceramic to metal (GCM) seals. Generally the glass ceramics exhibit a wide range of thermal expansion coefficient depending upon the composition and the presence of relative proportions of the crystalline phases. In a recent paper Shennawai et al. [8] carried out some studies to see the effect of a nucleating agent on the crystalline-phases developed and on thermal properties of Li_2O – MgO – Al_2O_3 – SiO_2 glass and glass ceramic. Similar studies have also been reported by Donald et al. [9] and Demirkesen and Haytalman [10] on lithium zinc silicate glass-ceramics. Donald et al. [9] discussed the effect of composition including the influence of a nucleating agent on crystallization behaviour and on the thermal and mechanical properties of the resultant glass ceramics. However, the consolidated study of thermal expansion coefficient, glass transition temperature and micro hardness of MAS glass ceramic as a function of processing temperature seems to have not been reported. In addition, although, the general procedure for preparation of such technologically important material is available in literature, the crucial process parameters are either kept vague or missing. Therefore, this becomes an important part of any investigation.

In this communication we report the preparation and study of TEC, glass transition temperature, micro hardness etc. of MAS glass and glass ceramics having different compositions, prepared under different processing conditions. The concentration of MgF_2 nucleant was varied from 0 to 13.2 mol%. Due to the multicomponent nature of the material, the behaviour has been found to be somewhat complex. The average TEC (30–300 °C) and T_g of base glass samples decrease from 8.38 to $7.936 \times 10^{-6}/^\circ\text{C}$, and from 653.55 to 599.8 °C, respectively, with increase in MgF_2 content. The micro hardness of base glass without MgF_2 is higher (6.822 GPa) as compared to 13.2 mol% MgF_2 (6.32 GPa). However, in all the cases TEC increases and micro hardness decreases when glass is transformed to a glass ceramic by controlled crystallization at different processing temperatures (max 1050 °C). The results have been explained on the basis of the role of Mg in the glass matrix and that of fluorine in the formation of crystalline phases and microstructure of the glass ceramic material.

2. Experimental

The MAS glass ceramic samples with different compositions were prepared by following the glass route, using a four-stage heating schedule, involving calcination, glass formation (melting and quenching), nucleation and crystallization. The details of the procedure have been reported elsewhere [11]. The initial charge was prepared by taking analytical grade chemicals in the form of oxides/carbonates of Si, Al, B, K and Mg. Magnesium fluoride was used as the nucleating agent. The nominal compositions of different batches are given in Table 1. We prepared samples by keeping the ratio of silica to total metal oxides of Al, B, K and Mg to about 1.13 and varied the content of MgF_2 from 0 to 13.2 mol% (batches I, II and III). In order to study the effect of Mg, we also prepared samples (batch IV) in which MgO content was doubled in the base composition of batch II. In the first stage the charge was mixed thoroughly and calcined at 950 °C for 24 h with a predetermined heating schedule. The calcined charge was melted in a closed Pt-10%Rh crucible at 1450–1500 °C for 2–4 h in a raising and lowering hearth furnace (model 'OKAY' 70R10, M/s Byshakh and Co., Kolkata) and poured into a graphite/brass mould of max. 75 mm dia and 30 mm height. This was immediately transferred to an annealing furnace maintained at around 500 °C for 4–6 h. After annealing the glass was cooled to room temperature at the rate of 20 °C/h. In order to transform the glass to a glass ceramic, controlled nucleation and crystallization were carried out in a programmable vertical tubular furnace using different heating schedules. For nucleation, the temperature of the sample was varied from 550 to 600 °C for 4–6 h and for crystallization from 750 to 1050 °C. These temperatures were based on DTA data [11]. The sample was cooled to room temperature at the rate of 60 °C/h. A number of samples were prepared with different heating schedules.

The bulk density of the sample was measured at room temperature by the liquid displacement method (Archimedes method) with the accuracy of measurement of ± 0.05 g/cc. Crystallization and phase formation were identified by the powder diffraction method employing CuK_α radiation from an X-ray diffractometer (Rikagu,

Table 1
Nominal composition of different batch samples

| Batch | $\text{SiO}_2/\text{M-Oxide}$ | MgO (mol%) | MgF_2 (mol%) | T_g (°C) (base glass) | Avg. TEC ($10^{-6}/^\circ\text{C}$) (base glass) |
|-----------|-------------------------------|---------------|--------------------------|----------------------------|---|
| Batch I | 1.137 | 12.85 | 0.00 | 653.55 | 7.937 |
| Batch II | 1.127 | 12.85 | 6.6 | 610.8 | 8.35 |
| Batch III | 1.129 | 12.85 | 13.2 | 599.8 | 8.38 |
| Batch IV | 0.764 | 25.7 | 6.6 | 664.9 | 7.25 |

$$\text{M} = \text{Al} + \text{B} + \text{K} + \text{Mg}.$$

Japan model D-4000). The scanning was done in the range of $2\theta = 20-70^\circ$.

The thermal expansion coefficient measurements were carried out in a dilatometer (model- TMA/92 Setaram, France) using a silica probe. The heating rate was kept to $10^\circ\text{C}/\text{min}$ for all measurements. The size of the samples was kept at a max. of 20 mm height and 10 mm diameter with both ends flat. The samples were kept in a quartz sample holder with a constant load of 5 g for all measurement. Before starting the experiment the chamber was evacuated up to 10^{-2} mbar pressure and then the chamber was flushed with high purity (IOLAR grade) Ar gas. All the measurements were carried out in flowing Ar atmosphere with a constant flow rate of 40–50 l/h. The temperature was varied in the range of 30–580 $^\circ\text{C}$ for α measurement. The expansion coefficient being reported is the average in the temperature range of 30–300 $^\circ\text{C}$. The micro hardness of the sample was measured by indentation technique using Vickers indenter on the micro hardness tester (model VMHT 30M, Leica). Before measurements, the sample surface was polished with $0.3\text{ }\mu\text{m}$ alumina powder to get good reflective surface. The measurement was done by applying a 100 g load for 5 s. An average of at least 10 readings was taken.

The surface finish of the sample was measured on a Profilometer (Taylor Hobson Surtronic-3 model) by the LVDT method. For this purpose, the sample was first

machined on a conventional lathe (maximat) using carbide tipped tools and then polished with $0.3\text{ }\mu\text{m}$ Al_2O_3 powder for 1 h before the measurement. The scanning electron microscopy (SEM) was employed for studying the microstructure. For this measurement, gold coating was given by vacuum evaporation/deposition on a naturally fractured surface etched with 5% HF solution. The measurements were done on a SEM model: Stereoscan S-240, Cambridge, UK.

3. Results and discussions

The densities of base glass samples of different batches were found to be in the range of 2.50–2.6 g/cc and those of glass ceramic samples in the range 2.51–2.78 g/cc. The densities for different glass and glass ceramic samples are summarized in Tables 2–5.

Fig. 1(a) shows the XRD patterns for batch I samples processed at different temperatures. It is clear that no crystalline phase has developed up to 850 $^\circ\text{C}$ processing temperature as expected. Absence of the nucleating agent would require a rather higher temperature for inducing nucleation and subsequent growth. The predominant phase developed in these samples was magnesium silicate of low concentration at processing temperature above 850 $^\circ\text{C}$.

Table 2

Different measured parameters for batch I samples of MAS after processing at different temperatures

| Process temperature ($^\circ\text{C}$) | Density (g/cc) | Average TEC (30–300 $^\circ\text{C}$) ($10^{-6}/^\circ\text{C}$) | Micro hardness (GPa) |
|--|--------------------|---|----------------------|
| – | 2.501 ^a | 7.936 ^a | 5.84 ^a |
| 600 | 2.509 | 7.936 | 5.84 |
| 725 | 2.507 | 8.211 | 5.74 |
| 850 | 2.5123 | 8.266 | 5.67 |
| 950 | 2.5139 | 8.413 | 5.57 |
| 1050 | 2.5359 | 8.6 | 5.43 |

^a Measured values for base glass.

Table 3

Different measured parameters for batch II samples of MAS after processing at different temperatures

| Processing temperature ($^\circ\text{C}$) | Density (g/cc) | Average TEC (30–300 $^\circ\text{C}$) ($10^{-6}/^\circ\text{C}$) | Micro hardness (GPa) |
|---|-------------------|---|----------------------|
| – | 2.55 ^a | 8.35 ^a | 6.12 ^a |
| 600 | 2.553 | 8.53 | 6.03 |
| 725 | 2.555 | 9.255 | 5.82 |
| 850 | 2.557 | 9.553 | 5.74 |
| 950 | 2.568 | 9.592 | 4.59 |
| 1050 | 2.612 | 9.618 | 4.25 |

^a Measured values for base glass.

Table 4

Different measured parameters for Batch III samples of MAS after processing at different temperatures

| Processing temperature ($^\circ\text{C}$) | Density (g/cc) | Average TEC (30–300 $^\circ\text{C}$) ($10^{-6}/^\circ\text{C}$) | Hardness (GPa) |
|---|--------------------|---|-------------------|
| – | 2.605 ^a | 8.38 ^a | 6.32 ^a |
| 600 | – | 9.285 | 6.32 |
| 725 | – | 9.56 | 6.25 |
| 850 | – | 9.821 | 5.02 |
| 950 | – | 9.873 | 4.67 |
| 1050 | 2.67 | 10.159 | 4.22 |

^a Measured values for base glass.

Table 5

Different measured parameters for batch IV samples of MAS after processing at different temperatures

| Processing temperature ($^\circ\text{C}$) | Density (g/cc) | Average TEC (30–300 $^\circ\text{C}$) ($10^{-6}/^\circ\text{C}$) | Micro hardness (GPa) |
|---|--------------------|---|----------------------|
| – | 2.593 ^a | 7.25 ^a | 6.86 ^a |
| 600 | – | 7.463 | 6.82 |
| 725 | – | 7.583 | 6.34 |
| 850 | – | 9.376 | 5.22 |
| 950 | – | 9.587 | 5.37 |
| 1050 | 2.781 | 9.643 | 5.36 |

^a Measured values for base glass.

The XRD patterns for the samples of batch II are shown in Fig. 1(b). In this case the noticeable crystalline phases were developed only at 850 °C. They were identified as norbergit and magnesium fluorosilicate. At a

higher temperature (950 °C) the fluorophlogopite phase with a trace of magnesium silicate phase developed and above 950 °C there is some tendency of decomposition of the fluorophlogopite phase that favours the growth

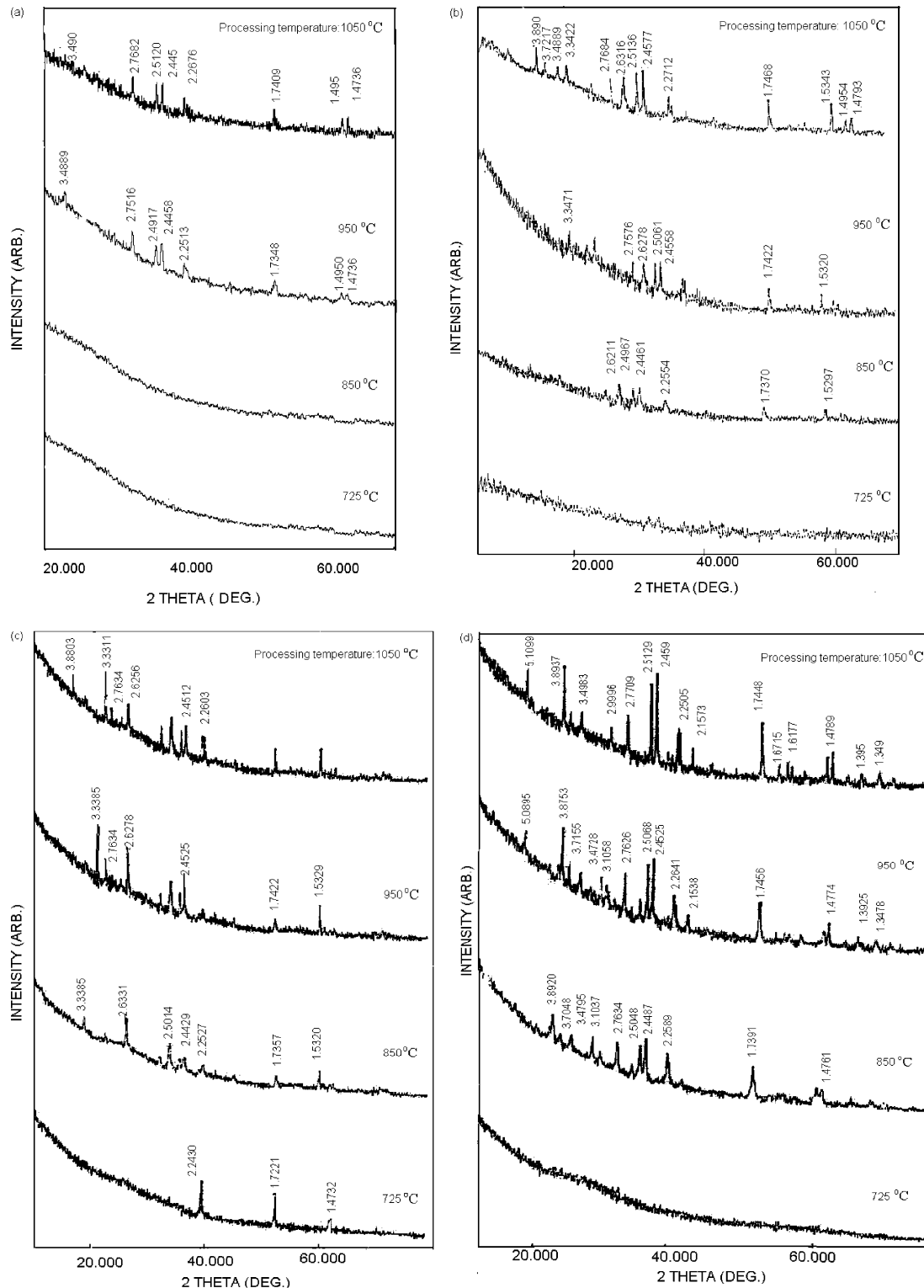


Fig. 1. (a) XRD patterns at different processing temperature for batch I. (b) XRD patterns at different processing temperature for batch II. (c) XRD patterns at different processing temperature for batch III. (d) XRD patterns at different processing temperature for batch IV.

of magnesium silicate phase [12]. In this case, the replacement of the fluorine ion ($r=1.36 \text{ \AA}$) with oxygen ion ($r=1.4 \text{ \AA}$) breaks the continuous glass network forming a pair of $\Xi \text{ Si-F}$ [13] to balance the charge of oxygen ion, which helps in atomic rearrangement conducive to growth of crystalline phases. Fig. 1(c) shows the XRD patterns of the samples for batch III processed at different temperatures. The crystalline phases were noticed after 725°C processing temperature. They were identified as a major fluorophlogopite phase mixed magnesium fluorosilicate phase. This shows that as the concentration of fluorine increases with an increase in the MgF_2 content, the growth of fluorophlogopite phase gets favoured even at a lower temperature. Since, with increase in the MgF_2 concentration, there is a reduction in viscosity, which increases the mobility of ions thus, able to produce required super saturation for nucleation and growth at low temperatures.

The XRD patterns of batch IV samples processed at different temperatures are shown in Fig. 1(d). There is no observable crystalline phase formation up to 725°C and above this temperature predominantly a magnesium silicate phase is developed. It is believed that the increase in MgO/SiO_2 ratio allows Mg to go into the glass network. This alters the normal structure and increases the probability of growth of a magnesium silicate phase. When the processing temperature is increased,

there is more growth of magnesium silicate as evident from the increase in the intensity of related peaks.

Linear expansion i.e. displacement per unit length as a function of temperature for different base glass samples are reproduced in Fig. 2. The average TEC ($30\text{--}300^\circ\text{C}$) and T_g deduced from these curves are included in Table 1. Glass transition temperatures of base glasses decrease and thermal expansion coefficients increase with the increase in the content of MgF_2 . On the other hand, glass transition temperatures of the base glasses increase and thermal expansion coefficients decrease with the increase in the content of MgO . The average TEC of base glass seems to be dependent on the content of Mg. The sample having maximum Mg concentration shows the lowest TEC. It seems that as the MgO/SiO_2 ratio increases, a more rigid glass network is formed (evident from the high value of T_g i.e. 664.9°C for batch IV), which increases the bond strength and decreases the local vibration -O- resulting in low TEC.

The thermal expansion coefficients for different batch samples after processing at different temperatures are found out and are summarized in Tables 2–5. Dependence of average TEC ($30\text{--}300^\circ\text{C}$) as a function of processing temperatures for all the batches is shown in Fig. 3. The TEC of the base glass of batch I ($7.936 \times 10^{-6}/^\circ\text{C}$), increases rather slowly with processing temperature, reaching to $8.6 \times 10^{-6}/^\circ\text{C}$ at 1050°C . It is

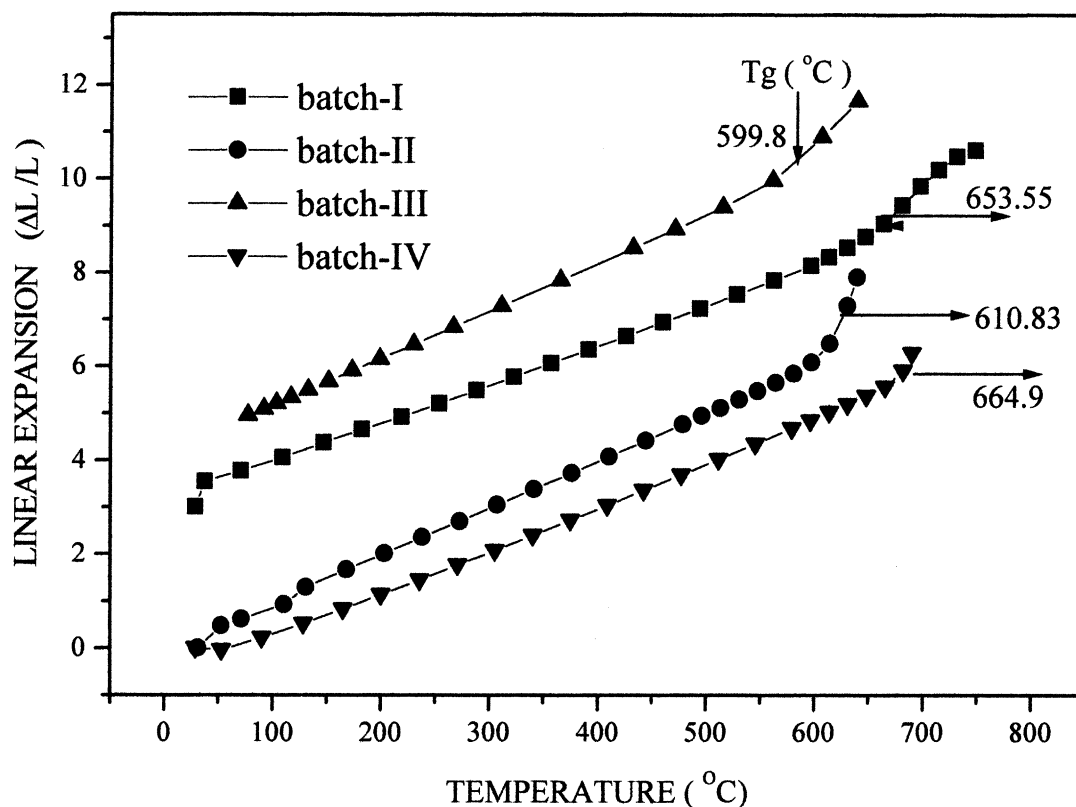


Fig. 2. Linear expansion vs temperature of base glass for batches I–IV. The curves for batches I and III are displaced by 3 and 5 units, respectively for clarity.

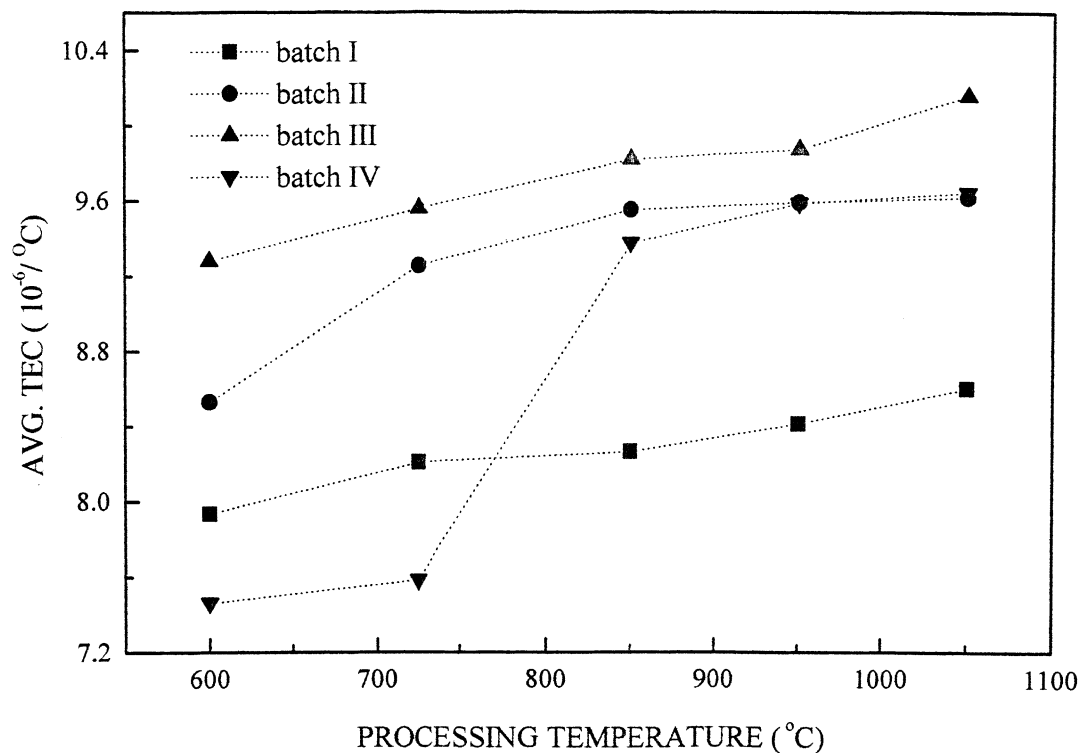


Fig. 3. Average thermal expansion coefficient vs processing temperatures for batches I–IV.

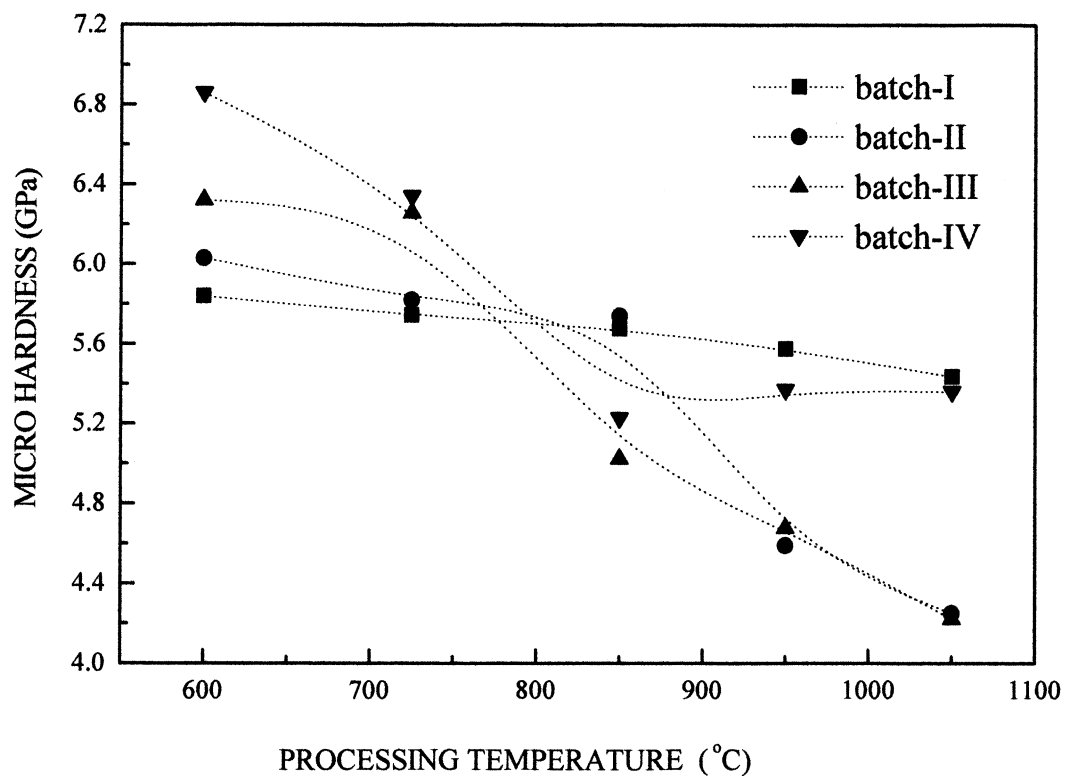


Fig. 4. Microhardness vs processing temperatures for batches I–IV.

interesting to note that, although XRD measurements do not show any crystalline phase formation up to 850 °C, there is an increase in TEC. This might be due to molecular/atomic rearrangements in the material due to processing temperature.

TEC of the base glass of batch II is found to be $8.35 \times 10^{-6}/^{\circ}\text{C}$, which gradually increases to $9.6 \times 10^{-6}/^{\circ}\text{C}$ after processing at 1050 °C. This increase in TEC is due to formation of different crystalline phases at different processing temperatures. The TEC of the base glass of batch III is about the same ($8.38 \times 10^{-6}/^{\circ}\text{C}$) as for batch II and also follows the similar dependence of TEC with processing temperature but has a higher basic TEC. This is thought to be due to a higher percentage of fluorophlogopite phases formed due to a increased content of the nucleating agent. The TEC batch IV samples varies in a somewhat complex manner as evident from Fig. 3. There is a slow increase up to 725 °C and then it rises sharply to $9.37 \times 10^{-6}/^{\circ}\text{C}$ at a processing temperature of 850 °C and again attains a value $9.643 \times 10^{-6}/^{\circ}\text{C}$ after processing at 1050 °C. However, a sharp rise in TEC is due to the formation of the Mg_2SiO_4 phase, which has a higher thermal expansion coefficient [14].

Dependence of micro hardness on processing temperatures for different batch samples is shown in Fig. 4. The micro hardness for the batch I base glass sample is 5.85 GPa which decreases slowly to 5.43 GPa after processing at 1050 °C. The decrease in hardness results from the presence of a magnesium silicate phase as confirmed by XRD. In the case of batch II samples the micro hardness of base glass (6.128 GPa) decreases marginally with processing temperatures up to 850 °C and then rather sharply to 4.258 GPa at 1050 °C. The decrease in micro hardness is due to the formation of planner plate-like fluorophlogopite crystallites above 850 °C as is clear in SEM micrograph reproduced in Fig. 5. This type of structure has a tendency of plastic

flow/deformation under load. The dependence of micro hardness on processing temperature for batch III shows first a gradual decrease up to 725 °C and then a sharp decrease to a value of 4.221 GPa at 1050 °C. This is thought to be due to the formation of planner fluorophlogopite phases, above 725 °C as mentioned earlier. The micro hardness for the batch IV glass sample (6.861 GPa) is rather high because of high Mg content. However, it reduces to 5.22 GPa at 850 °C where the Mg_2SiO_4 phase is formed. Further increase in temperature does not have a significant effect on the hardness.

The machinability for all different batch glass ceramic samples was tested with a conventional technique using carbide tipped tools. Although all samples were showing machinability with a spindle speed of 54-sfm and cutting angle of 5°, increase in MgF_2 concentration had a direct effect on surface finish and ease of machining. Increased amount of MgF_2 helped in developing more of the fluorophlogopite phase with the desired plate-like crystallites of 4–5 μm (Fig. 5). This seems to help in producing a surface with minimum asperities/irregularity on machining. Thus MgO and MgF_2 have different roles to play and affect the properties in somewhat complex manner. MgF_2 affects not only the TEC, and helps crystallization but also plays a crucial role in modifying the microstructure.

4. Conclusions

We have produced good quality machinable MAS glass ceramic having TEC of about $9.6 \times 10^{-6}/^{\circ}\text{C}$. The characteristics such as surface finish, TEC, micro hardness, etc. of a glass ceramic needed to ascertain machining and sealing, depend upon the phase developed. The increase in Mg content favours the formation of a magnesium silicate phase while an increase in fluorine (MgF_2) content improves the machinability through the formation of a more fluorophlogopite phase and modifying the microstructure. In addition, the glass transition temperature depends upon the content of Mg affecting the glassy network. MAS NMR study on base glasses might throw some more light on this aspect. Having made high voltage insulators/spacers for UHV application [11], we are now working on the optimization of the process for making glass ceramic to metal seal with metals/alloys like AISI 446 (28%Cr–Fe) having TEC of $10.2 \times 10^{-6}/^{\circ}\text{C}$.

Acknowledgements

The authors wish to thank Dr. V.C Sahni, Director, Physics Group and Head, TP& PED, for his constant support and encouragement to this work. Our thanks are due to Dr. S.C Sabharwal for providing the XRD

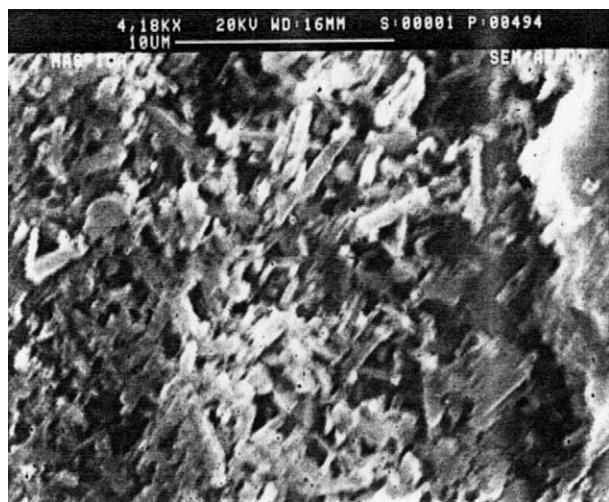


Fig. 5. SEM photograph of batch III glass ceramic sample processed at 1050 °C.

facility. We would also like to thank Mr. J.K. Panchal and Mr. K M Bandal for carrying out the machining of the glass ceramics.

References

- [1] D.G. Grossman, Machinable glass–ceramics based on tetrasilicic mica, *J. Am. Ceram. Soc.* 55 (1972) 446–450.
- [2] D.S. Baik, K.S. No, J.S. Chun, Mechanical properties of mica glass–ceramics, *J. Am. Ceram. Soc.* 78 (5) (1995) 1217–1222.
- [3] D.S. Baik, K.S. No, J.S. Chun, Y.Y. Yoon, H.Y. Cho, A comparative evaluation method of machinability of mica based glass ceramics, *J. Mater. Sci.* 30 (1995) 1801–1806.
- [4] D.S. Baik, K.S. No, J.S. Chun, H.Y. Cho, Effect of the aspect ratio of mica crystals and crystallinity on micro hardness and machinability of mica glass ceramics, *J. Mater. Process.* 67 (1997) 50–54.
- [5] T. Hoche, S. Habelitz, I. Avramov, Crystal morphology engineering in $\text{SiO}_2\text{--Al}_2\text{O}_3\text{--MgO--K}_2\text{O--Na}_2\text{O--F}^-$ mica glass ceramics, *Acta. Mater.* 47 (3) (1999) 735–744.
- [6] S. Habelitz, G. Carl, C. Russel, S. Thiel, U. Gerth, J.-D. Schnapp, Mechanical properties of oriented mica glass ceramic, *J. Non-Cryst. Solids* 220 (1997) 291–298.
- [7] Lj. Radonjic, Lj. Nikolic, The effect of fluorine and concentration on the crystallization of machinable glass–ceramics, *J. Eur. Ceram. Soc.* 7 (1991) 11–16.
- [8] A.W.A. El-Shennawi, A.A. Omar, A.R. El-Ghannam, Expansion characteristics of some $\text{Li}_2\text{O--MgO--Al}_2\text{O}_3\text{--SiO}_2$ glasses and glass ceramics, *Ceram. Int.* 17 (1991) 25–29.
- [9] W. Donald, B.L. Metcalfe, D.J. Wood, J.R. Copley, The preparation and properties of some lithium zinc silicate glass ceramics, *J. Mater. Sci.* 24 (1989) 3892–3903.
- [10] E. Demirkesen, E. Maytalman, Effect of Al_2O_3 addition on the crystallization behavior and bending strength of a $\text{Li}_2\text{O--ZnO--SiO}_2$ glass–ceramics, *Ceram. Int.* 27 (2001) 99–104.
- [11] M. Goswami, T. Mirza, A. Sarkar, M.S. Sangeeta, S.L. Verma, K.R. Gurumurthy, V.K. Shrikhande, G.P. Kothiyal, Preparation and characterization of magnesium–aluminium–silicate glass ceramics, *Bull. Mater. Sci.* 23 (2000) 377–382.
- [12] E.A.A. Mustafa, Fluorophlogopite porcelain based on talc–feldspar mixture, *Ceram. Int.* 27 (2001) 9–14.
- [13] P.W. McMillan, Process of controlled crystallization, in: *Glass-Ceramics*, Academic Press, London, 1964, p. 72.
- [14] J.D. Cawley, W.E. Lee, Oxide ceramics, in: M. Swain (Ed.), *Structure and Properties of Ceramics*, in: R.W. Cahn, P. Hassen, E.J. Kramer (Eds.), *Material Science and Technology*, vol. 11, 1994, p. 69.